Proceedings World Geothermal Congress 2020+1
Reykjavik, Iceland, April - October 2021

Protective Iron Boride Coatings against Corrosion in Geothermal Wells

Eugene Medvedovski

71, 4511 Glenmore Trail SE, Calgary, Alberta, T2C 2R9, Canada

eugenem@endurancetechnologies.com, emedvedovski@shaw.ca

Keywords: Protective coatings, Iron Boride, Corrosion, Scaling, Geothermal conditions

ABSTRACT

The challenges facing production equipment in geothermal processing, e.g. piping systems, in terms of corrosion, and the causes of failures and degradation of steels used for processing equipment components are analyzed. As one of the surface protection options, to minimize these problems and to enhance the equipment performance, iron boride coatings obtained through thermal diffusion process are proposed. The principles of formation of the iron boride coatings on steels produced by Endurance Technologies Inc. (ETI) are reported. As opposed to many coating technologies, the ETI thermal diffusion process provides high integrity of finished products without spalling and delamination on the entire working surfaces of components. The results of testing in different corrosion environments are presented. The boride-based coatings with two-layer dense microcrystalline structures successfully withstand the actions of high temperature / high pressure water and steam with a presence of H_2S, $CO+CO_2$, chlorides, hydrocarbons in simulating conditions tested in the autoclave and in the pressurized Atlas cell, as well as in strong acidic environments. These coatings also demonstrated minimal scaling and corrosion when the materials were immersed into the model mixes of chloride salt solutions with SiO_2 or $SiO_2+Fe_2O_3$ at elevated temperatures and into the brine solution at boiling. Iron boride coatings also have high hardness and wear resistance in sliding sand flows. Complex-shape and long components (tubing up to 12-m length) with inner or inner and outer protected surfaces can be manufactured, which will promote significant extension of the steel service life in harsh geothermal-related corrosion or corrosion-abrasion environments.

1. INTRODUCTION

The power that can be obtained through geothermal sources is a CO_2-free heat source with a high potential globally. As opposed to many renewable energy sources, its output is independent from weather conditions and from day-night-rhythm. This power generation route is attracting high attention in Europe, North America and other continents as a reliable and rather inexpensive option (often more affordable than fossil fuel alternatives) without hazardous gases emission. Geothermal heat can be used directly or through the heat exchangers for the heating of the residential, agricultural and industrial units and facilities, as well as for electricity generation when high temperature (>150^{o}C) steams from the hot fluids are used to spin turbines [DiPippo, 2015; Finster et al, 2015].

One of the main challenges in exploiting of geothermal energy is severe deterioration and failures of the metallic components of processing equipment resulting from their corrosion by geothermal fluids with very complex hydrochemistry and due to other very harsh service conditions [Ellis et al, 1977; Miller, 1980]. In fact, nearly all naturally occurring elements of the Periodic Table ranging from Hydrogen to Uranium can be found in the geothermal fluids. Numerous organic and inorganic compounds comprising CO_2, hydrocarbons, H_2S and other S-based substances, ammonia, carbonic acids, chlorinated hydrocarbons, various salts (especially, chlorides) and others may also be present there depending on the geological conditions of the source environment, which majority of them promote severe corrosion of steels [Bai et al, 2014, Choi et al, 2011; Corsi, 1986; Zheng et al, 2017; Linter et al, 1999; Lopez et al, 2003; Grafen et al, 1996; Anderko, 2004]. Such highly corrosive geothermal fluids are prone to cause scaling inside various components and piping where fluids and gases are transported, and this scaling reduces processing flows creating additional turbulence and related erosion issues. High temperatures and pressures naturally involved in the geothermal conditions strongly increase corrosion and related failures of the production components. In many situations, corrosive media act synergistically with abrasive particles flows, which significantly facilitate the destruction of production components. The level of corrosion and scaling problems depend on geological and environmental conditions, as well as geothermal production/ processing features, such as hydrogeochemistry and geology, water reservoir depth and related temperature/pressure in the wells, composition of materials in the geothermal facilities, type and design of the wells, flow rate, operating parameters, and many other factors [Gallup, 1998; Mundhenk et al, 2013; Klapper et al, 2016; Boch et al, 2017]. Mineral precipitation and scaling intensity vary in a great extent depending on the geological features. However, according to numerous studies, the major scaling issues occur due to the presence of silica and silicates, clay materials, calcium carbonate and dolomite, as well as sulfates, hydroxides and chlorides salts [Gallup, 1998; Boch, 2017; Zarrouk et al, 2014; Wolfgramm et al, 2011]. Corrosive conditions in aquifers and geothermal wells result in the formation of metal (mainly, iron) sulfides, sulfates, carbonates and hydroxides, which also significantly increase the scaling issues [Corsi, 1986; Regenspurg et al, 2015, Valdez et al, 2009; Bai et al, 2014].

Many geothermal processes require well (downhole) pumps, circulation pumps, piping systems, heat exchangers, convectors, condensers where the major components are usually made of steels and alloys, which have limited performance under severe service actions. It should be noted that, in many production situations, the tubing and casing strings should work at high depths reaching of a few kilometers [Thorbjornsson et al, 2015; Lichti et al, 2015], and service in the wells with such depths generally requires elevated pressures and temperatures during production and where geothermal fluids are more corrosive with presence of abrasive suspended solids and precipitants. Because of that, the production and processing equipment should be made from the reliable materials, which should withstand the actions of corrosive geothermal fluids and gases, high temperatures (up to 400^{o}C) and pressures, erosion and friction, and their combination, and where the scaling issues are minimized.

Despite numerous research projects conducted during recent decade, appropriate material selection with respect to corrosion resistance, sensitivity to scaling, workability and cost remains a real challenge at the present time [Miller, 1980; Zarrouk et al, 2014; Mundhenk et al, 2013]. Basically, two common approaches for materials selection are used for production components: low-cost materials with frequent replacement in case of failure and corrosion resistant materials which serve longer but which are significantly more expansive. Mainly steel materials, from carbon steels to different stainless steels, and Ni- and Ti-based alloys are considered for these applications [Kaya et al, 2005; Karlsdottir et al, 2013; Lichti et al, 2015, Thorbjornsson et al, 2015]. Thus, carbon steels and high strength low-alloy steels mostly employed in downhole equipment, similarly to mineral oil exploration and production, are low cost materials, but have limited resistance to corrosion and scaling. Their poor performance (failures) leads to frequent replacement of equipment components and associated downtime and high processing cost. At the other hand, high alloyed steels, such as stainless steels and duplex steels, and Ni- or Co-rich alloys offer significantly higher corrosion resistance and lower susceptibility to scaling but are very expensive, and they would not have adequate performance if corrosion and wear situations occur synergistically. Expensive materials such as tantalum (Yusoff et al, 2011) and titanium alloys (MacDonald and Grauman, 2019) find application in acid solutions and high temperature brines respectively. Polymeric materials have a very limited potential in this field because of a poor resistance to elevated pressures and temperatures. Thus, thermosetting and thermoplastic and other polymeric coatings have mediocre performance and may be used at temperatures only up to 200^{o}C [Muller et al. 2010; Belas-Dacillo et al, 2015; Schreiber et al, 2013], which is very similar to performance of such coatings for downhole oil production. Although clad materials have been also considered, the results of their evaluation have not been convinced so far. Also, these materials are not suitable for long tubing. Hence, there is an urgent need for the cost-competitive and reliable technical solution for the geothermal processing, specifically for high temperature applications for electricity generation, e.g. inexpensive but corrosion resistant materials for piping and other parts in the fluid transferring systems. Materials surface engineering, particularly, protective coatings on steels, can be a straightforward route to improve performance of the materials and products involved in the geothermal processing. Different coating materials and technologies, including electrolytic- or electroless–based processes, cold and thermal spray coating processes, painting and spin coating and many other chemical and mechanical coating processes may be considered [Roberge, 2012; Wang et al, 2009; Cha et al, 2002; Movchan et al, 2014; Chicatun et al, 2007; Musil et al, 2008; Heath et al, 1997; Mittemeijer et al, 2014]; however, many of them cannot be used either due to their lower performance in high temperature corrosive-erosive conditions or due to low probability to apply them for protection of long tubing and other large size and complex shape production components.

Surface engineering through the thermal diffusion process can be considered as a highly promising technology to protect steel components against corrosion and corrosion-wear at elevated temperatures. This technology is based on the principles of chemical vapor deposition (CVD), but, as opposed to conventional CVD, it is more versatile and cost effective due to no need of special CVD chambers with complicated maintenance and no insertion of special reactive gases, which are often expensive and hazardous. This process includes the immersion of the steel components into special powder mix and their heating to certain temperatures when the reactive gas occurs due high temperature reactions in this mix. Due to high temperature reactions, certain elements occur in the gas phase and deposit onto the steel surface with their diffusion into the steel surface and consequent interaction with the major constituents of steel (e.g. Fe, Cr, Ni). The inward diffusion of the desired elements and outward diffusion of Fe and other constituents of steel and formation of intermetallides with their consolidation result in the formation of the protective coatings on steel components when this coating becomes the integral part of the steel components. According to these principles, coatings based on iron borides, aluminides, chromides, silicides and some other intermetallides can be obtained. The details of this process (also called diffusion alloying and pack cementation) were described elsewhere [Davis, 2001; Dearnley, 2017; Nicholls, 2000; Mittemeijer et al, 2014; Bangaru et al, 1984; Meier et al, 1989; Medvedovski, 2016]. Among these thermal diffusion coatings, the coatings consisting of iron borides onto steels have a great potential owing to their high corrosion resistance and wear resistance [Telle et al, 2000; Campos-Silva et al, 2010; Petrova et al, 2007; Tabur et al, 2009; Martini et al, 2004]. In this case, the boronizing process includes the formation of the B-based gases at high temperature when B atoms deposit onto and diffuse into the steel structure with formation of iron borides and consequent consolidation of the formed structure. High application properties of boronized steels are defined by the high values of thermodynamic properties of iron borides (e.g. high crystalline lattice energy and enthalpy) and strong, short covalent bonds of Fe-B [Matkovich, 1977; Samsonov et al, 1976; Kunitskii et al, 1971; Gordienko, 2002] when these properties are directly related to high chemical inertness and high hardness of these compounds [Cheetham et al, 1991; Donald et al, 2005]. A total coating thickness (case depth) is usually in the range of 100-250 μm (for carbon steels and low-alloy steels), which can be directionally managed by the process parameters at the boronizing. The iron boride coatings demonstrate high wear resistance, e.g. in friction, abrasion and erosion conditions, and withstand the action of corrosive environments, such as strong acids, salts, water steam with a presence of corrosive gases at elevated temperatures and pressures [Medvedovski et al, 2014; Medvedovski, 2016]. These coatings are already successfully used to protect various steel components, including long tubing with inner or inner and outer surface protection, for downhole oil production, refinery and some other industrial applications where high temperature corrosion, wear and their combination are the major factors negatively affecting the performance of steels [Medvedovski et al, 2014; Medvedovski, 2016, Medvedovski et al, 2016].

The present work is devoted to consideration, for the first time, of the iron boride-based coatings for protection of steels against corrosion and scaling in the geothermal high temperature conditions and their testing in these conditions, e.g. in high temperature – high pressure water and steam with a presence of corrosive gases, and in a contact of salts at elevated temperatures of the conditions simulating the geothermal situations. There are no dedicated standardized methods to evaluate corrosion and scaling resistance of the materials for geothermal applications. In fact, the testing methods on corrosion resistance in general should be a simulating response, more or less, to some application/ service conditions, which vary depending on particular situation. In many cases, weight change and electrochemical methods (e.g. electrochemical impedance spectroscopy and potentiodynamic polarization) are employed for the corrosion level characterization; however, they only indicate the changes occurring with the surface of the materials under certain conditions but do not show what happens with the material structure and composition, i.e. without integrity consideration, and do not indicate if the formed corrosion products are protective or not. The compositional and structural analyses, both cross-sectional and surface examination, should be considered as very important, and they have been employed in the present study for preliminary evaluation of corrosion and scaling for the proposed coating in comparison with bare steels.

2. EXPERIMENTAL

2.1 Materials and Processing

Low carbon steels widely used for the tubular products for oil and gas and geothermal applications were selected for the present studies. In particular, steel J55 as a tubular material and steel A36/44W as a flat bar, both with carbon contents in the range of 0.2-0.3% and identical properties, were used as the substrate material for boronizing and as a bare steel (hereafter "CS"). The boronized steel samples (denoted as "B-CS") were prepared according to the proprietary Endurance Technologies Inc. (ETI)' technology. Briefly, this technology included preparation of the steel samples, their blasting or treatment with sandpaper, degreasing and immersion into the specially formulated boronized powder mix. The ETI boronizing mix (pack) consisted of the B-rich ingredient, salt activator and inert material with a special ratio between the ingredients and with specially selected particle sizes, which provided the required processing characteristics. The steel samples immersed into this boronizing mix were placed into a retort (container), and then the sealed retort was heated in a conventional electric kiln at the predetermined temperature (ranging of 800 - 1100°C) for the predetermined time. Upon the heat treatment, the iron boride protective coating was formed [Medvedovski et al, 2014]. After the cooling of the kiln, the samples were taken from the retort and cleaned from the processed boronizing mix.

2.2 Corrosion Testing

Corrosion testing in the high temperature – high pressure conditions was conducted in the autoclave system (see Fig. 1). The autoclave and piping were made of Hastelloy C276 and stainless steel 316L materials. The system consisted of the autoclave connected with the gas supplying vessels, compressor and pressure gage, the vent system and the pressure and temperature regulators. The flat bar samples with dimensions of approximately (125-150)x25x6.3 mm were partially immersed into water contained 1.5% NaCl and 1.5% $CaCl_2$, so this setting allowed exposure in the corrosive liquid – gas conditions. The gas medium consisted of steam with 0.3% H_2S, 12.6% hydrocarbons, 17.7% CO and 69.4% CO_2. Temperature and pressure were 280°C and 28 MPa, respectively. These conditions were selected based on general consideration of the geothermal corrosive environments, e.g. in California (USA) and in Alberta (Canada), and the autoclave capability. The autoclave test was conducted for 7 days. Since it is well known that corrosion of carbon steels and low-alloy steels actively occurs in the water-steam conditions, especially in the presence of CO_2, H_2S and other gases, at temperatures above 100°C even at low pressures [Linter et al, 1999; Lopez et al, 2003; Bai et al, 2014; Choi et al, 2011] and since the considered high pressure – high temperature conditions with the presence of corrosive gases is significantly more severe than "common" high temperature water and steam, it was decided to test only the samples with the iron boride coatings at the mentioned conditions.

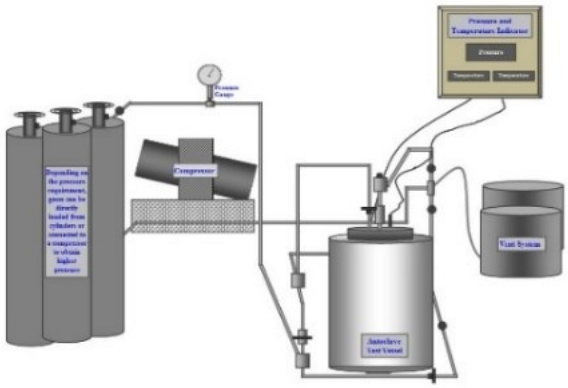

Figure 1: Principle schematic of the high temperature – high pressure autoclave system (left).

Figure 2: Testing unit for corrosion in hot acids (right).

2.2.1 Boiling strong acid testing

Behavior of boronized steel (as well as 304 and 316 stainless steels for comparison) in acids was studied using HCl and H_2SO_4 solutions having 15% and 70% concentration, respectively. Boiling points of the acids would have been of the order 105 °C for 15% HCl and 160 °C for 70 % H_2SO_4 The samples (~77x25x6.4 mm) were almost completely immersed into and heated to 100°C in a sealed vessel (Fig. 2) using a Teflon holder for standing. During the tests (7 days or 168 hrs.), the samples were periodically observed with their weight and dimensions measuring and weight loss calculation.

2.2.2 High temperature boiling salt solutions testing

Corrosion-scaling testing was conducted in the contact with model mixes containing chloride salts of alkali and earth-alkali metals. The compositions of the model mixes were selected based on the average data from the geothermal wells located in California (USA). The mix compositions G1 and G2 are presented in Table 1. The samples (bare carbon steel and steel with the iron boride coating) with configuration of "square tube" with rounded corners having outer size of ~24x24 mm, ~3 mm of wall thickness and length of ~25 mm were placed onto one side onto refractory support, and approximately equal quantities of the model salts were placed onto one side of the inner surface of the "square tube". The samples were placed into the tube electric kiln, which was heated to 370°C for 2 weeks and then the temperature in the kiln was increased to 416°C. Each group of the samples (CS-G1, B-CS-G1, CS-G2, B-CS-G2) was exposed to the action of the salt mix and oxidation at elevated temperature for 1-2-3-4 weeks, when the samples of each group were withdrawn from the kiln every week.

In parallel, the samples (bare carbon steel and steel with the iron boride coating) with the same configuration were partially immersed in the "muds" prepared by blending of the model salt mixes (G1 and G2) with water at concentrations less than sea water according to the schematic shown on Fig. 3. The ceramic (porcelain) crucibles with the muds and samples were covered by a loose fitting refractory plate lid and heated to 370°C into electric kiln for 1 week. In this case, the samples were exposed to the scaling-corrosion action of the boiling salts (at an estimated temperature of 110 °C), and steam at elevated temperature.

Table 1. Modeling mix compositions (wt.-%) for the scaling-corrosion test.

Mix	NaCl	KCl	$CaCl_2$	$BaCl_2x2H_2O$	LiCl	SiO_2	Fe_2O_3	$CaCO_3$
G1	54.0	16.6	28.4	0.2	0.3	0.5	-	-
G2	53.4	16.5	28.0	0.2	0.3	0.5	1.1	-
G3	52.1	16.2	27.2	0.2	0.4	1.1	1.4	1.4

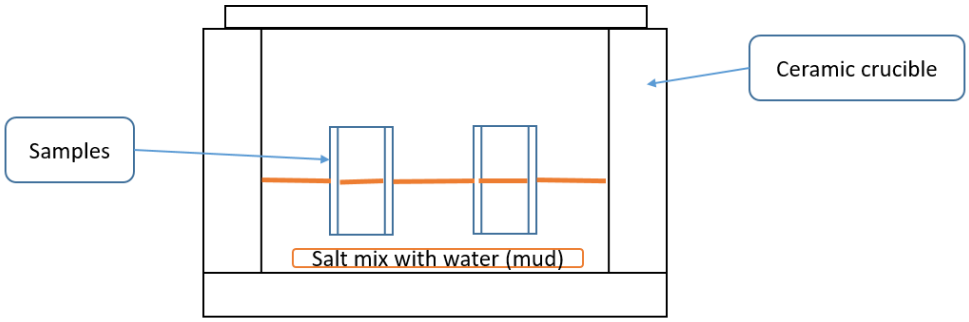

Figure 3: Schematic of the scaling-corrosion testing at elevated temperature.

The samples (bare carbon steel and steel with the iron boride coating) with the same configuration but with a length of ~50 mm were also tested under the boiling conditions in the model mixes G2 and G3 (Table 1). Thus, these mixes were blended with water in a ratio of salt : water at (12-15) : (88-85), the samples were partially submerged into the boiling suspensions and exposed in the containers with closed lids for ~4 + 7 hrs. with periodical refilling the containers to maintain the submerging level, i.e. the samples were exposed to the action of salts and water at 110 °C and steam at elevated temperature.

2.3 Materials Examination

After the testing, the samples were visually examined for color, presence or absence of scale, flakes, delamination, micro-cracks and pitting. Then the samples were rinsed with water and dried and visually inspected again. After that, they were weighed using a digital balance with an accuracy of ±0.01 g. A relative mass change was calculated as $(\Delta m/m_0).100\%$ in [%], or a corrosion rate was calculated as $\Delta m/(\rho.S.t)$ in [cm.hr^{-1}], where Δm is mass change, ρ is density, S is surface area, t is test duration.

The examination of the cross-sections was performed with light optical microscope MEIJI Techno 1M7200 to observe possible changes of the coating structures after corrosion/ scaling testing and to determine thicknesses of the coating layers or the scale. For the samples' preparation for the cross-section microscopy examination, precision cutting-polishing multiple-step procedure established at ETI was employed using the Buehler equipment and diamond tooling. The special acidic-based etching composition (e.g. Nital consisted of the nitric acid solution in ethanol) was utilized to reveal the structural features in the cross-sections. The surface morphology was examined using Scanning Electron Microscope (SEM) JEOL JSM-IT300LV InTouchScope. The relative contents of the key elements at the coating were determined by X-ray energy dispersive spectrum (EDS) analysis using Oxford Instruments a JEOL JED-2300 DRY SDD EDS detector with INCA Suite 4.13 software; the quantities both in weight-% and atomic-% were determined. The XRD data were collected using a PANalytical Aeris X-ray diffractometer. Qualitative XRD analysis and Rietveld Refinement was performed using HighScore Plus XRD analysis software.

Micro-hardness determination of the iron boride coatings, as well as the steel substrate, was conducted according to ASTM E384 with the Clark micro-hardness tester CM400AT applying the Knoop diamond indenter to the polished cross-section at the load of 100 g (HK0.1) for 10-15 s. The Knoop hardness was calculated in accordance with formula:

$$HK = 14.229(P/d^2),$$

where P – force [kgf] and d – length of the long diagonal of the replica [mm] made at the indentation.

The Knoop micro-hardness testing method was selected, among other methods, as the most reasonable for the coatings of different thicknesses. In this case, the coating layers and the substrate can be examined by applying appropriate indentation load and compared under the same conditions. Since the corrosion and temperature affect, in general, stress and micro-crack formation, phase and microstructure modification or changes, and their level and rates depend on the material integrity, and since hardness also depends on the structure and presence of the defects, the hardness comparison should be valuable for better understanding of the corrosion resistance and integrity of the studied materials, in particular, of the considered coating.

3. RESULTS AND DISCUSSION

3.1 Material Properties of Coatings

The coating structure of the boronized samples had the specific "saw-tooth" morphology (see Fig. 4), which is identical to ones described in our earlier conducted works, as well as in other studies [Medvedovski et al, 2014; Medvedovski et al, 2016; Telle et al, 2000; Mittemeijer et al, 2014]. In this microcrystalline structure, the inner zone (which is closer to the substrate) mostly consists of the Fe_2B phase, and the outer zone mostly consists of the FeB phase. Thus, the FeB phase grows on the Fe_2B repeating the morphology of the Fe_2B phase. The XRD analysis was not conducted for the boronized samples in this work since the phase analysis of similar coatings were obtained earlier [Medvedovski et al, 2014]. Although the iron boride phases (FeB and Fe_2B) have different crystallographic structures and different values of coefficients of thermal expansion, there were good bonding between the "layers" and with the steel substrate with no delamination and microcracks between the phases. Both protective layers are diffusion-bonded between each other and with the steel substrate. No mechanical interface between the boride coating and the substrate, and no Kirkendall porosity were observed. The details of the coating formation and coating composition have been described earlier [Medvedovski et al, 2014; Medvedovski, 2016]. The total case depth of the prepared iron boride coatings was around 200-220 µm or 155-165 µm. It should be noted that, with regards to case depth determination, it was measured from the top of the coating surface to the middle of the "teeth". The described structure and case depth are inherent to the entire treated surface of the boronized steel samples. Micro-hardness HK0.1 of the iron boride coating determined for the middle of the coating (the indenter was applied onto the middle of the cross-section) was in the range of 1700-1850 kgf/mm^2. The notable deviation between hardness data for different indentations is defined by the point that the sharp indenter could be applied either on the FeB or Fe_2B phases, which distinguish in hardness (FeB has higher hardness compared to Fe_2B). Thus, the Fe_2B phase usually has micro-hardness of 1600-1700 HK0.1 while the micro-hardness of the FeB phase usually ranges as 1750-1850 up to 1900 HK0.1 [Medvedovski et al, 2014]. No attempt was made to pre-select which phase the indenter was located in, and this gave some variation in before and after exposure results.

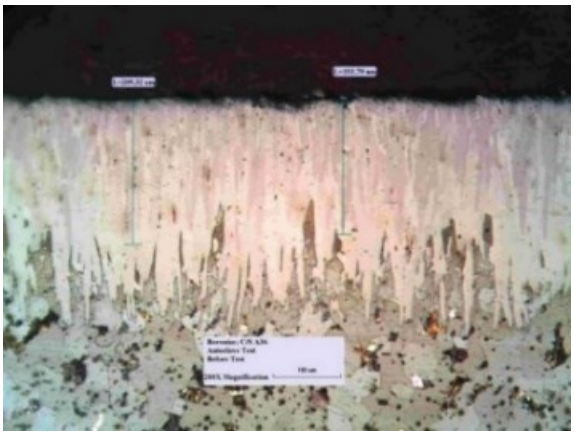

Figure 4

3.2 Exposure Testing Results

3.2.1 Steam and water pressure vessel results

The boronized steel samples did not have visual destruction and deterioration after the corrosion autoclave testing in the high temperature – high pressure environment contained steam of water with chloride salts and corrosive gases, such as CO_2, CO, H_2S and hydrocarbons. No delamination, spalling, pitting, bubbling or surface cracks were observed. Only surface discoloration could be noted that may be related to oxidation of iron boride just on the surface. The appearance of the samples can be seen on Fig. 5. The samples had minimal mass change that was <0.05%. Since the mass change was negligible and no delamination or flaking were detected, the formed "oxidation skin" may be considered as protective.

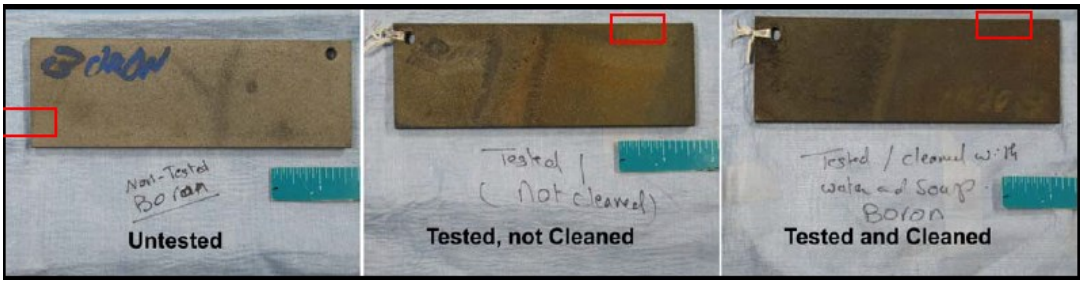

Figure 5. Appearance of the boronized samples before and after autoclave corrosion testing (red rectangles show locations for preparation of cross sections).

Microstructure of the boronized samples examined after the autoclave testing remained on the original level; no visible surface micro-cracks and caverns were observed (Fig. 6). Micro-structure was examined in three different zones, such as bottom (this part of the sample was completely submerged into the liquid), top (when the surface of the sample was affected by the corrosive gases) and middle area (where the surface was under liquid and gas simultaneously). The case depths of all zones remained on the original level that confirms high resistance of the iron boride coating in the selected high temperature – high pressure steam – corrosive gases

conditions. Only the surface of the samples became a little bit rougher. A thin "skin" with a thickness of a few microns can be observed on the micrograph related to the top zone of the boronized sample. This "skin" may be related to the surface oxidation of the iron boride coating. Since no noticeable destruction of the coating and no case depth reduction were observed, this "skin", which is probably amorphous iron boron oxide, may be considered as protective. No presence of S, Cl, Na and Ca was detected by the EDS analysis; only elevated content of O was detected that confirms oxidation of FeB. The data of micro-hardness HK0.1 also confirm high integrity of the iron boride coatings – micro-hardness of each zone (bottom, top and middle) was in the range of 1700-1850 kgf/mm^2, i.e. remained at the original level. These results supplement and are in agreement with the earlier obtained data on the corrosion resistance of this type of coating in the autoclave and pressurized Atlas cell testing in high temperature – high pressure steams contained corrosive gases (H_2S, CO_2 and hydrocarbons) simulating oil production conditions [Medvedovski, 2016].

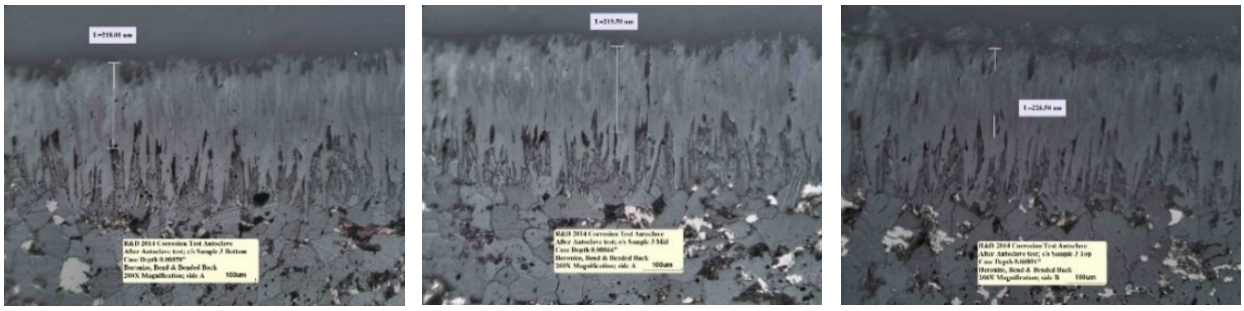

Bottom zone Middle zone Top zone

Figure 6. Microstructure of the cross-sections selected from the bottom, middle and top zones of the boronized steel after autoclave testing.

3.2.2 Boiling strong acid test results

The corrosion testing results obtained after exposure of the samples in hot acidic solutions are shown on Fig 7. The boronized carbon steel samples lost <1% of their weights after the 1-week exposure with no visible delamination of the coating, with no pitting, bubble formation or surface cracking. However, bare stainless steel samples experienced notable dissolution in the acids with a weight loss ~10% in HCl (for both steels) and ~6.5% for SS316 and ~23.5% for SS304 in H_2SO_4. Dissolution of stainless steels in HCl occurred quickly during the first 24-36 hrs. (calculated corrosion rate was ~0.44x10^{-3} cm.h^{-1}), and then the corrosion rate became significantly smaller (0.015 – 0.020)x10^{-3} cm.hr^{-1}. In the case of H_2SO_4, dissolution behavior of stainless steels was more complicated. Thus, corrosion was very intensive during 3rd-4th days; however, the corrosion rate during the next days was less but still high as 0.1x10^{-3} for SS316 and even 2x10^{-3} for SS304. As opposed to stainless steels, the corrosion rate for boronized carbon steel was significantly less, only 0.005x10^{-3} (in HCl) and 0.01x10^{-3} cm.hr^{-1} (in H_2SO_4) at the last stage of testing. Corrosion of the iron boride coating occurs through surface micro-cracks. The SEM images of the surface morphology of the samples SS316 and B-CS after testing in hot acids can be seen on Fig 8. The EDS analysis showed only traces of Cl and S on the surface of the boronized samples.

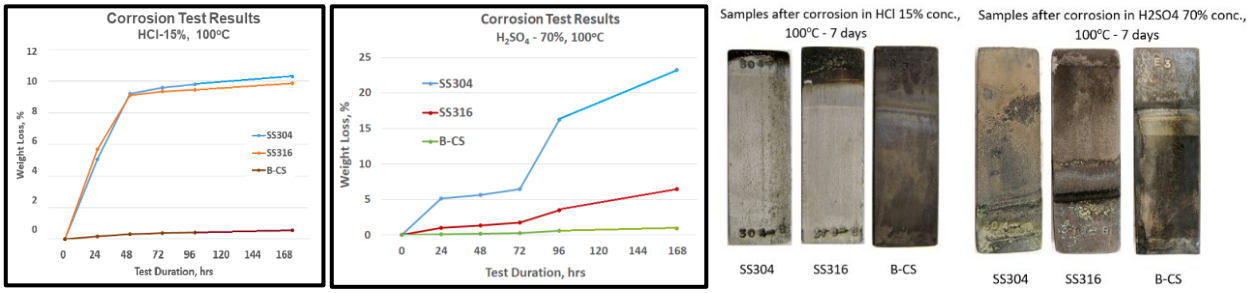

A) B) C) D)

Figure 7. Weight loss and appearance of the samples after 7 days exposure in HCl (A, C) and H_2SO_4 (B, D) at 100°C.

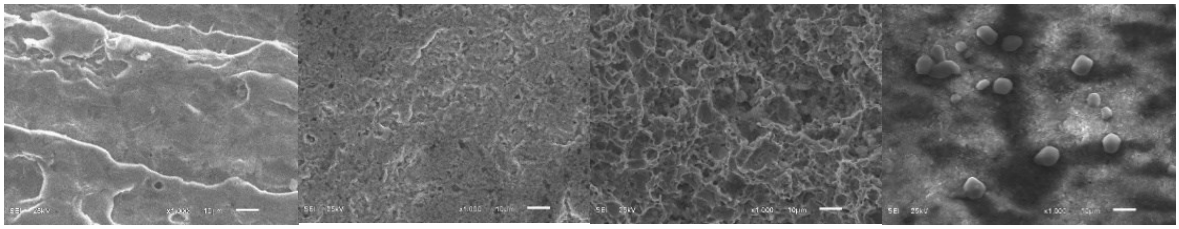

A) B) C) D)

Figure 8. Surface morphology of the samples after testing in hot acids.

Note for Figure 7 and Figure 8:

SS316 in HCl; B) B-CS in HCl; C) SS316 in H_2SO_4; D) B-CS in H_2SO_4

3.2.3 High temperature boiling salt solutions test results

After the scaling – corrosion testing the samples made of bare steel and made with the iron boride coating distinguish significantly (see Fig. 9). The deposition of the model salt solutions was greater in the case of bare steel. This difference was especially clear when the samples were immersed into the salts and exposed at high temperature. Thus, the boronized samples could be easy cleaned (rinsed with water) from the residue of the salts, and their surface became smooth. For these samples, the areas which were in contact with the "muds" and which were only under oxidation, had some difference in colors that is explained by surface oxidation. As opposed to the boronized steel, strong scale remained on the bare steel samples after washing even with a brush. Also, some peeling of the scale contained flakes of rust and even small metallic fragments from steel could be observed that indicates rather intensive interaction between the high-temperature salts and steel. At the same time, peeling of the oxidized scale (rust) occurred for the steel areas, which were not immersed into the salts, i.e. for the areas which were not in a direct contact with the salts. Both areas of bare steel samples (immersed into the "mud" and exposed to humid air) became notably rougher.

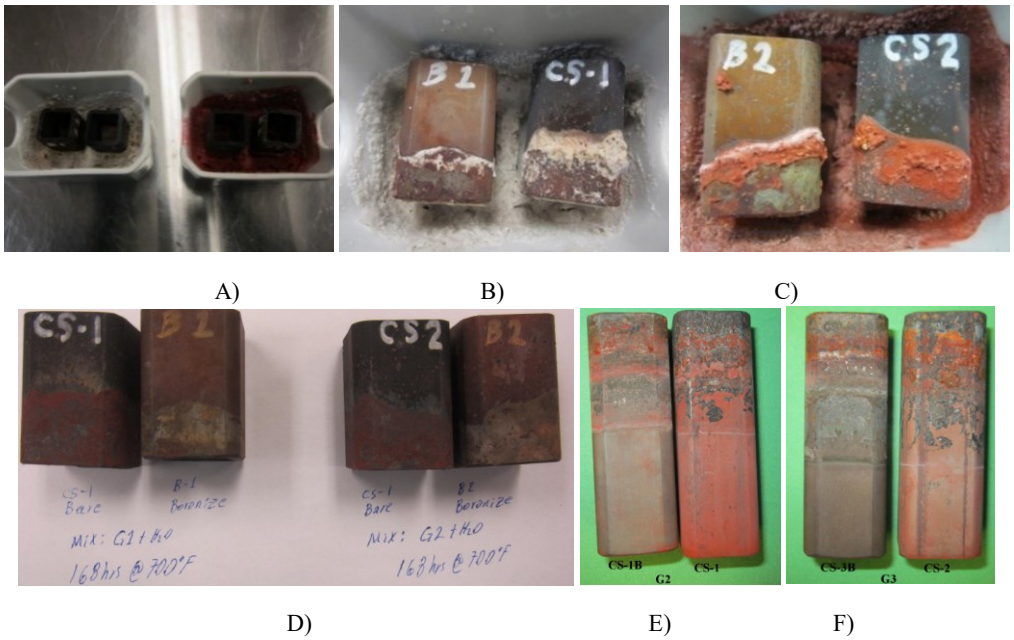

Figure 9. Appearance of the samples after scaling-corrosion testing in the model salt mixes (samples were immersed into the "mud"); test duration 168 hrs.

Samples into the crucibles; B) Samples after testing in the mix G1; C) Samples after testing in the mix G2; D) the same samples after testing and washing; E) and F) Samples after boiling tests in the suspensions G2 and G3

The data of the mass (weight) change for the bare steel and boronized steel samples confirm the difference in their behavior under scaling-corrosion conditions (Fig. 10). The mass of the bare steel samples grew with continuation of exposure under oxidation and salt, and it rose with a temperature increase. Comparing the results obtained after the boiling test, it may be assumed that the suspension G3 affected scaling and corrosion more than the suspension G2 (higher mass gain). However, because of flaking of the rust (occurred due to oxidation) and peeling of the part of scale "bonded" to the steel, the mass dropped, i.e. the mass change cannot be considered as a right and the only "tool" for the materials evaluation. Regarding the boronized samples, the mass change was significantly less compared to bare steel, and the mass change occurred under the scaling – air dry exposure was slower (in the case of salt mix G1) or even without growth (in the case of salt mix G2). The mass change may be more related to the surface oxidation of iron boride. In the case of immersion of the samples into the "mud", the slight mass loss was observed for the boronized samples.

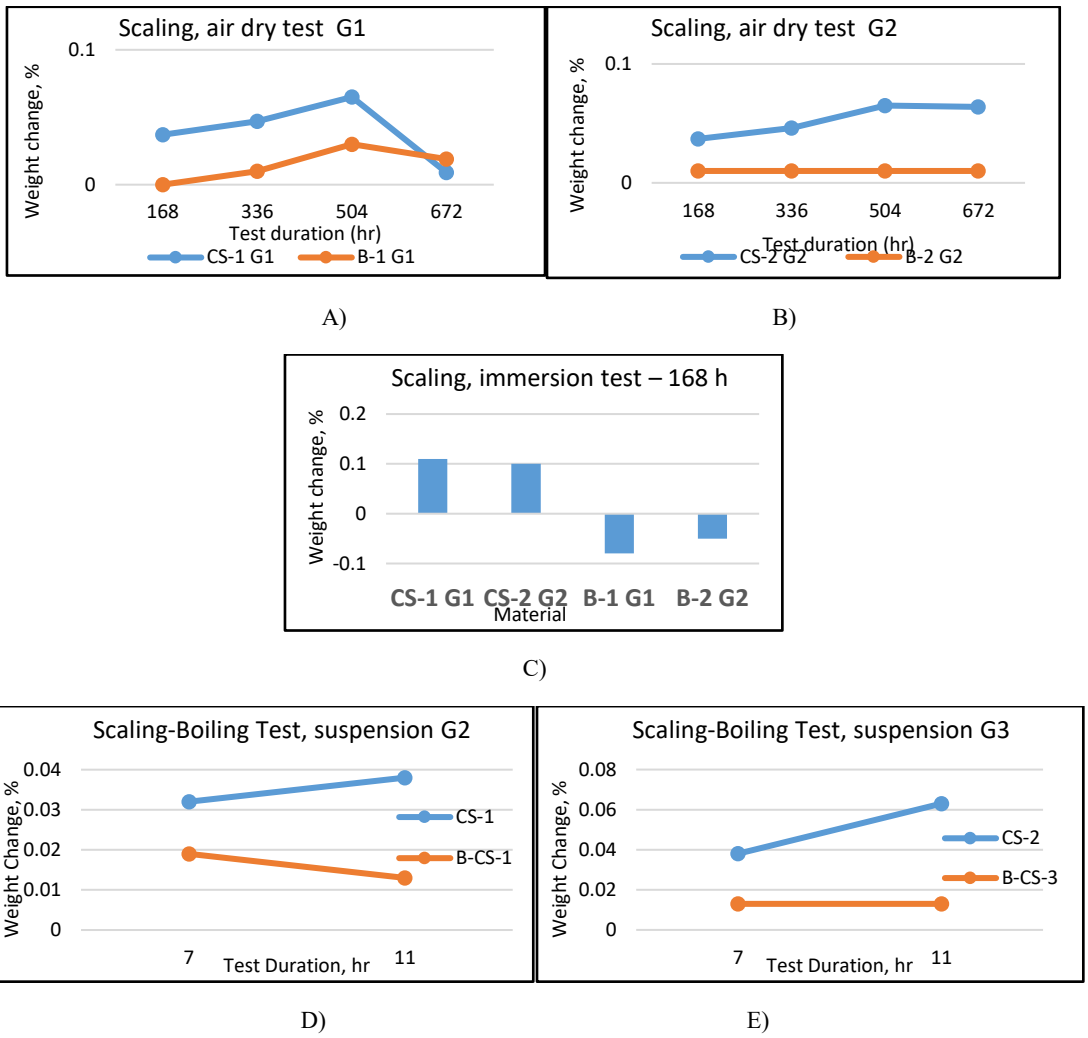

Figure 10. Mass (weight) change for the samples after scaling-corrosion testing.

Samples tested in contact with salt G1 in air at high temperature; B) Samples tested in contact with salt G2 in air at high temperature; C) Samples tested by immersion into salts ("muds") G1 and G2 at high temperature; D) Samples tested in boiling in G2 suspension; E) Samples tested in boiling in G3 suspension

The most important results related to the scaling-corrosion resistance of steels without and with protective iron boride coating were obtained from the studies conducted under microscope. Thus, bare carbon steel samples experienced strong interaction with the salts and formation of scaling (Fig. 11A and 11B). When the bare steel samples were prepared for the microstructure examination, the part of scale and rust was flaked off during cutting and polishing. However, the thickness of the scales achieved 75 -150 µm when the samples were exposed into the "muds" at elevated temperature. This formed scale was soft and brittle. Also, the rust formation of the steel and its partial peeling can be related to oxidation and decarburization of the steel surface.

In the case of testing of the samples with iron boride coating, no scale was observed under microscope. The microstructure of the coating remained on the original level (the coating thickness was ~200 µm for the samples designated for testing in the high temperature dry conditions and for the immersion into the salty "muds", and it was ~155-165 µm for the samples designated for the boiling test); no delamination, cracking and chipping, no pitting and no case depth reduction were observed (Fig. 11C and 11D). Micro-hardness of the coating also remained on the original level, i.e. in the range of 1650-1850 HK0.1. This data remains on the same level regardless the option of scaling-corrosion testing (i.e. dry air high temperature, boiling in the salt mix suspensions, and immersion into the salty "muds") that confirms a high integrity of the coating in the scaling-corrosion high temperature environments.

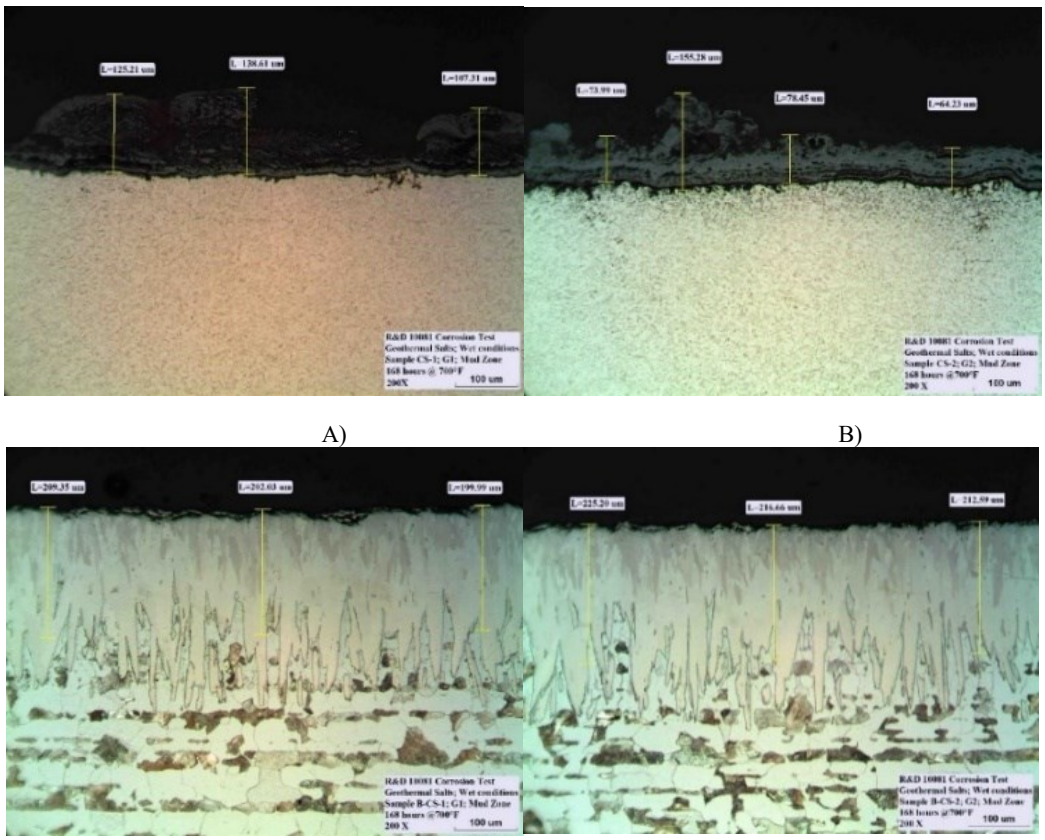

A) B)

C) D)

Figure 11. Microstructure (cross-section) of the samples exposed in contact with modeling mixes (immersion) at elevated temperature for 168 hrs. (magnification 200x).

Carbon steel, mix G1; B) Carbon steel, mix G2; C) Boronized steel, mix G1; D) Boronized steel, mix G2

The studies under SEM also confirm a presence of scales on the surface of carbon steel contacted with the "muds" G1 and G2 (Fig. 12 and 13). In some areas, silica grains with a well-defined structure are distributed among the scale (Fig. 12C). In addition, some peels were well adhered to the salt "mud" that can be especially noted for the sample contacted with the mix G2 (Fig. 13C). Surface oxidation with related decarbonization signs, partial peeling-off and pitting can be noted for the bare steel samples. The surface of the boronized samples remained on the original level. Only the signs of oxidation could be detected; the slightly glassy surface can be noted for the sample which was in contact with the mix G2. However, no scale was observed on the boronized surface, and no surface cracking, chipping and pitting could be also noted (Fig. 12D, 12E, 13D and 13E).

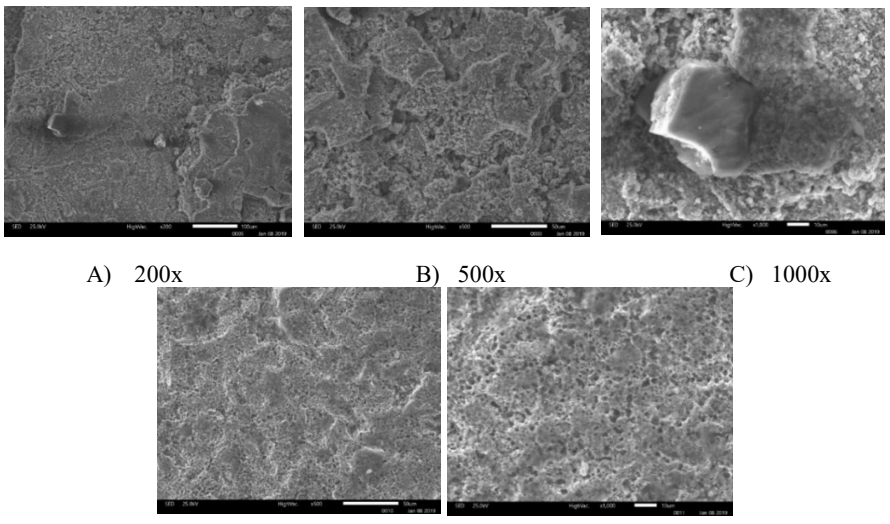

A) 200x B) 500x C) 1000x

D) 500x E) 1000x

Figure 12. SEM image from the surface of carbon steel (A, B, C) and boronized steel (D, E) after exposure in the G1 "mud".

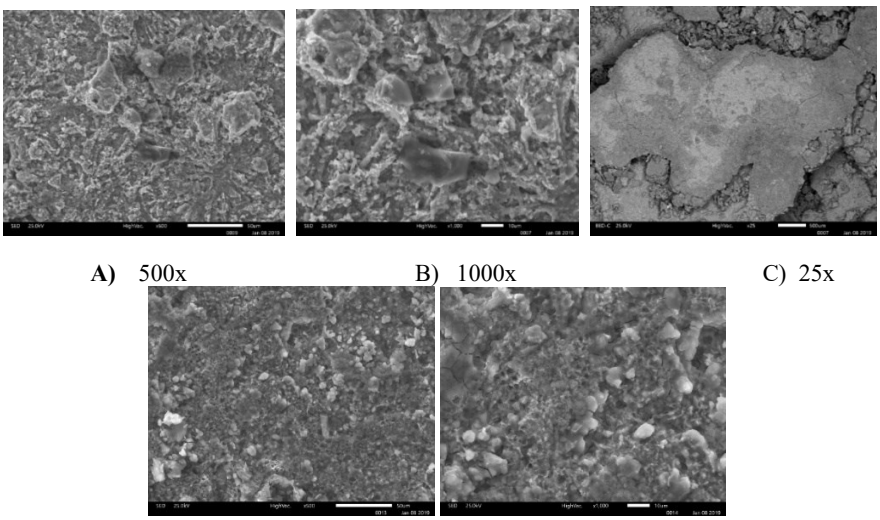

A) 500x B) 1000x C) 25x

D) 500x E) 1000x

Figure 13. SEM image from the surface of carbon steel (A, B, C) and boronized steel (D, E) after exposure in the G2 "mud".

The data of the EDS analysis confirm the interaction of the salts with bare steel and consequent scaling and pretty good resistance of the boronized steel in the considered environment. Thus, the data for carbon steel had rather big deviations that indicates of inconsistent distribution of elements on its surface and uneven oxidation (or, better to say, uneven peeling-off). The presence of some amounts of Cl, Ca, and Si could be detected. The analysis conducted for the grains clearly demonstrates the presence of silica adhered to the scale. Thus, bare steel samples experienced interaction with chlorides and scaling contained CaO and SiO_2, as well as strong oxidation with rusting and its peeling-off. As opposed to bare steel samples, the EDS analysis for iron boride coatings did not show sufficient presence of the elements from the salts, as well as SiO_2. Only elevated contents of oxygen for the boronized surface can be noted; as mentioned above, the boronized steel sample contacted with a salt G2 oxidized in a greater extent (a higher oxygen content on its surface). The data of the EDS analysis are summarized in Table 2. They show the data collected from the surface of the samples, as well as the data from the well detectable grains strongly adhered to the surface of bare steel.

Table 2. Results of EDS analysis (wt.-%) for the surfaces after exposure into the salt "muds" (370°C – 168 hrs).

Material	Fe	O	Ca	Si	Cl	B
CS-1 G1	68	28.5	0.4	0.3	2.1	-
grain	1.5	52.7		45.5		
CS-2 G2	70	27	0.2	0.2	2.1	-
grain	2.5	60.6		37		
B-CS-1 G1	77.3	12	0.1	0.08	0.08	9.5
B-CS-2 G2	60.5	29	0.2	-	0.1	9.6

The EDS analysis conducted for the flake collected from the exposed bare steel sample clearly showed interaction of the "mud" with steel and partial detachment of Fe together with the scale. This scale peeled-off from the sample CS-2 contacted with the mix G2 (see Fig. 10C) contains the following elements (wt.-%): Fe 25.5, O 25, Na 9, K 3.2, Ca 1.7, Cl 19.5, Si 0.1, C 5.5. Based on these data, it may be concluded that the salts strongly interacted with steel at elevated temperatures resulted in strong bonding between them, when the peeling had a big portion of Fe from the steel surface.

The XRD analysis conducted for the surface areas, which were in contact with the salt mixes ("muds") at elevated temperature showed the presence of iron-manganese $Fe_{0.969}Mn_{0.031}$, as well as magnetite, hematite and akaganeite β-$FeOOHxCl_n$, for the bare steel samples that confirms the corrosion and oxidation of the steel surface at the testing conditions. It should be noted that significant amounts of $Fe_{0.969}Mn_{0.031}$ on the surface analyzed can be explained by the peeling. Besides, some areas of the scale had quartz. In contrast, the XRD analysis conducted for the boronized samples did not show the presence of salts and other "new" phases; only iron boride phases (mainly FeB and small amounts of Fe_2B) remained on their surfaces. The formed iron boron oxide which may occur due to the surface oxidation is probably amorphous, and was not detected by XRD. The XRD results are presented on Fig. 14.

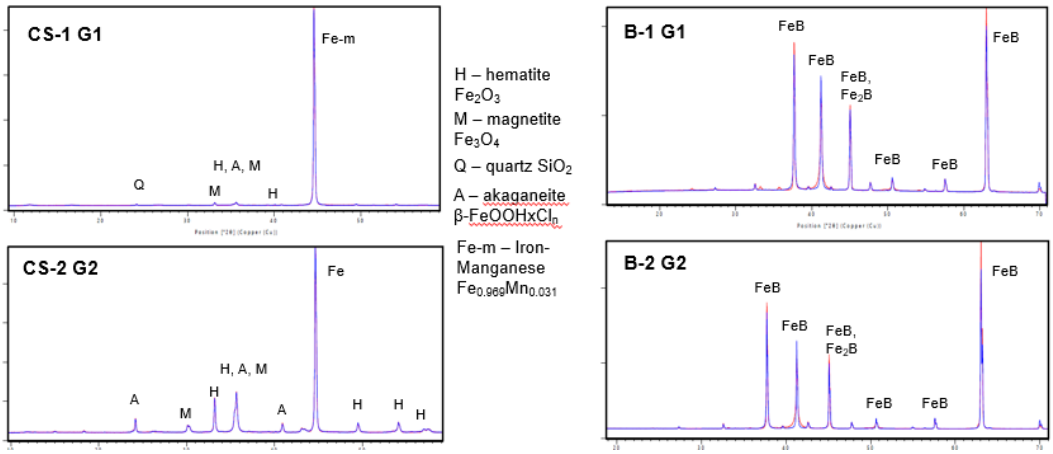

Figure 14. XRD results from the surface of the samples immersed into salt mixes ("muds") at 370ºC after 168 hrs.

Examination of the samples after the corrosion-scaling testing conducted under boiling of the brine-rich suspensions (with mixes G2 and G3) under microscope repeated the results described above. Carbon steel samples experienced corrosion and oxidation with formation of the scale of ~40-50 µm poorly adhered to the base material. It should to be noted that continuous boiling (i.e. agitation) promoted peeling of the formed scale, i.e. the scaling was uneven. In contrast, the boronized samples (the iron boride coating thickness was originally 155-165 µm) demonstrated high resistance to the mentioned boiling conditions; no coating thickness reduction, no micro-cracking and pitting were observed, and no scaling or deposition occurred on the boronized surface (Fig. 15). Again, only surface oxidation with a very thin oxide skin could be noted for these samples.

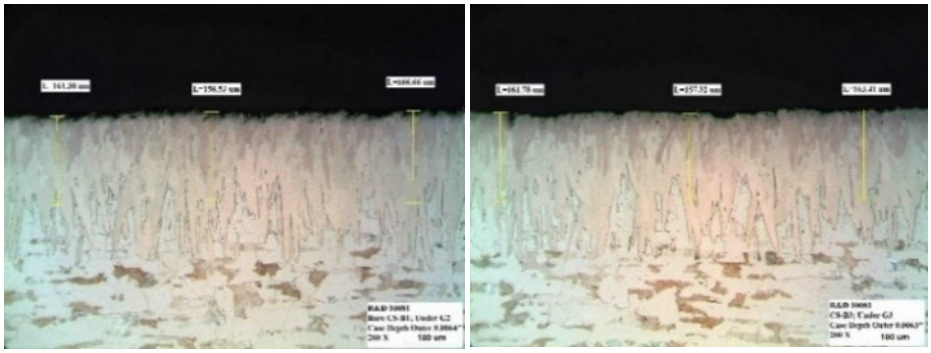

A) B)

Figure 15. Microstructure (cross-section) of the boronized samples after boiling in the water-based suspensions for 11 hrs. (magnification 200x).

Boronized steel, mix G2; B) Boronized steel, mix G3

4. SUMMARY OF RESULTS

According to the conducted testing in the high temperature – high pressure steam-gas conditions in the autoclave and in contact with salts at high temperatures (in dry, boiling and "mud" conditions), the iron boride coatings demonstrated rather high corrosion and scaling – corrosion resistance. It may be explained by well consolidated structure of the coating and by strong diffusion-related bonding to the substrate material. In fact, the coating has two layers, both consisted of the compounds with strong and short covalent bonds Fe-B and high thermodynamic properties, e.g. enthalpy, which, in general, provide high chemical inertness. While iron sulfides, iron carbonates and iron oxides (as soft and porous products, which are easy to peel-off) occur due to corrosion of steels during their contact with H_2S, CO_2 and H_2O at high temperatures and pressures [Choi et al, 2011; Bai et al, 2014; Boch et al, 2017; Linter et al, 1999; Lopez et al, 2003], and when chlorides cause the breakage of the passivating films on steels leading to intensive localized corrosion and pitting [Grafen et al, 1996; Anderko et al, 2004], no formation of these compounds were found in the case of iron boride coating. In the case of this coating, there are no "free" Fe that can start reacting with these gases, and the bonds of Fe-B are strong enough to prevent them to "break" as required to initiate these reactions. Similar explanation may be applied for possible contacts with Cl-based and other salts in geothermal fluids. The demonstrated results are a good addition to the obtained data related to the corrosion resistance of the boronized steels in oil production corrosive environments, e.g. in water steam with a presence of hydrocarbons and corrosive gases, at elevated temperatures and pressures, as well as in alkali salts [Medvedovski, 2016].

It might be expected that in highly oxidizing high temperature conditions, when iron boron oxide "film" occurs on the iron boride surface, the contact with silica and alkali and earth-alkali salts may result in further formation of a glassy "skin" promoting a scaling possibility. However, this issue did not occur, even when the samples were immersed into the salty "muds" and exposed at high temperature. As demonstrated, the microscopy and XRD studies confirmed the absence of visual scaling on the boronized samples. In these conditions, the surface oxidation was insufficient, and FeB did not react with SiO_2 and salts involved to the testing.

As indicated above, the proposed coating has a unique microcrystalline architecture which positively affects corrosion resistance. Both iron boride layers are diffusion-bonded, i.e. delamination between the layers in the case of their destruction is minimized. Two protective layers with sufficient thicknesses (totally greater than 150 μm) provide a high level of integrity in the considered testing conditions, and this structure is favorable not only in corrosive environments, but also in the situations, when some micro-cracks may occur during mechanical or thermal stresses in handling or service. The principle of steel protection with thermal diffusion coatings with this architecture was described in our earlier work [Medvedovski, 2016].

Although geothermal conditions may include the action of the corrosive flows rich with abrasive particles and friction-related conditions, the special wear-corrosion testing was not conducted in the present study. However, our previous works demonstrated high resistance of boronized steels and cast irons under combined actions of friction of steel bars in suspensions containing silica sand, NaCl and other salts and acids, as well as to the abrasive and erosive flows of silica-rich media [Medvedovski et al, 2014; Medvedovski et al, 2016], while bare steels experienced high wear-corrosion degradations even under shorter test duration. High wear- and wear-corrosion resistance of this coating is defined by high hardness of iron borides, which is significantly greater than of silica sand and similar materials. Because of that, it can be assumed that boronized steel would also have satisfactory performance under the combined action of corrosive media with abrasive particles related to geothermal applications. It should be noted that expensive stainless steels and Ni-rich alloys generally have low performance in abrasion or friction-related conditions since they have rather low hardness (lower than silica sand and similar materials), and their benefit of better corrosion resistance (despite significantly higher cost) compared to inexpensive carbon steels becomes negligible when the process occurs in a combination of wear and corrosion.

The coatings based on iron borides considered for the geothermal applications for the first time and tested in the simulating corrosion and scaling-corrosion conditions may be promising for protection of steel components for geothermal applications, especially for the high temperature conditions for electricity generation. Since corrosion resistance is defined by the composition and structure of the coating, the use of low-cost carbon steels with this coating may be an efficient and economical solution. These coatings can be successfully produced for components with different shapes and sizes, including for long tubing (up to 10-12 m length) and T- and Y-sections when the inner or inner and outer surfaces need to be protected.

5. CONCLUSION

The iron boride coating on low-cost carbon steel obtained through thermal diffusion technology was considered for the geothermal corrosion and scaling-corrosion application for the first time, and this coating demonstrated promising behavior in the conditions simulating some high temperature geothermal conditions. Thus, iron boride coating withstood the action of high temperature – high pressure steam contained sufficient amounts of corrosive gases, such as CO_2, CO, H_2S and hydrocarbons, had high resistance in hot concentrated acidic solutions (e.g. HCl and H_2SO_4) and did not demonstrate notable signs of scaling and corrosion when they were in contact with mixes of salts also contained SiO_2, Fe_2O_3 and $CaCO_3$. The coating structure remained well consolidated without thickness reduction, without cracking or delamination issues and without formation of "foreign" phases. The promising corrosion and scaling resistance of the coating is related to general inertness of iron borides, consolidated microcrystalline structure consisted of two protective layers with sufficient thickness greater than 100 μm and diffusion related bonding between the layers and with the steel substrate. The thermal diffusion technology is well suitable for protection of large size components, especially for protection of inner surface of long tubing which is a challenge for many other coating technologies. Because of the mentioned, the iron boride coatings can be recommended for longer and more extensive testing and evaluation in the corrosion-scaling geothermal related conditions, including using model and full size components. This consideration can be especially focused on the applications related to electricity generation where high temperatures combined with corrosive fluids and gases are involved and where bare steels have poor performance.

REFERENCES

Anderko, A., Sridhar, N., and Dunn, D.S.: A General Model for the Repassivation Potential as a Function of Multiples Aqueous Solution Species, *Corros. Sci.,* **46**, (2004), 1583-1612.

Bai, P., Zheng, S., Zhao, H., Ding, Y, Wu, J., and Chen, C.: Investigation on the Diverse Corrosion Products on Steel in Hydrogen Sulfide Environment, *Corros. Sci*., **87**, (2014), 397-406.

Bangaru, N.V., and Krutenat, R.C. Diffusion Coatings of Steels: Formation Mechanism and Microstructure of Aluminized Heat-Resistant Stainless Steels, *J. Vac. Sci. Technol. B,* **2:4**, (1984), 806-815.

Belas-Dacillo, K., de Leon, A.C., Panopio, A.C.R., and Advincula, R.C.: Evaluating protective coatings and metal alloys in acidic geothermal fluids using laboratory techniques, Proceedings World Geothermal Congress 2015, Melbourne, Australia, 19-25 April 2015.

Boch, R., Leis, A., Haslinger, E., Goldbrunner, J.E., Mittermayr, F., Froschl, H., Hippler, D., and Dietsel, M.: Scale-Fragment Formation Impairing Geothermal Energy Production: Interacting H_2S Corrosion and $CaCO_3$ Crystal Growth, *Geotherm Energy*, **5:4**, (2017), 1-19.

Campos-Silva, I., Ortiz-Dominguez, M., Bravo-Barcenas, O., Doñu-Ruiz, M.A., Bravo-Bárcenas, D., Tapia-Quintero, C., and Jiménez-Reyes, M.Y.: Formation and Kinetics of FeB/Fe_2B Layers and Diffusion Zone at the Surface of AISI 316 Borided Steels, *Surf. Coat. Technol.*, **205:2**, (2010), 403-412.

Cha, S.C., Gudenau, H.W., and Bayer, G.T.: Comparison of Corrosion Behaviour of Thermal Sprayed and Diffusion-Coated Materials. *Mater. Corros*., **53:3**, (2002), 195-205.

Cheetham, A.K., and Day, P.: Solid State Chemistry: Techniques, Oxford Science Publications: Oxford, UK, (1991)

Chicatun, F., Cho, J., Schaab, S., Brusatin, G., Colombo, P., Roather, J.A., and Boccaccini, A.R. Carbon Nanotube Deposits and CNT/SiO2 Composite Coatings by Electrophoretic Deposition, *Adv. Appl. Ceram*., **106:4**, (2007), 186-195.

Choi, Y.S., Nesic, S., and Ling, S.: Effect of H_2S on CO_2 Corrosion of Carbon Steel in Acidic Solutions, *Electrochim. Acta*, **56**, (2011), 1752-1760.

Corsi, R.: Scaling and Corrosion in Geothermal Equipment: Problems and Preventive Measures, *Geothermics*, **15**, (1986), 839-856.

Davis, J. (Ed): Handbook of Thermal Spray Technology, ASM International: Materials Park, USA, (2004), pp. 1-36

Dearnley, P.: Surface Engineering with Diffusion Technologies. In Introduction to Surface Engineering; Cambridge University Press, Cambridge, UK, (2017), 35-115

DiPippo, R.: Geothermal Power Plants: Evolution and Performance Assessment, *Geothermics*, **53**, (2015), 291-307.

Donald, H., and Jenkins, B.: Thermodynamics of the Relationship between Lattice Energy and Lattice Enthalpy. *J. Chem. Educ*., **82:6**, (2005), 950-952.

Ellis, A.J., and Mahon, W.A.J.: Chemistry and Geological Systems, Academic Press, New York, NY (1977).

Finster, M., Clark, C., Schroeder, J., and Martin, L.: Geothermal Produced Fluids: Characteristics, Treatment Technologies, and Management Options, *Renew Sust. Energ. Rev.,* **50**, (2015), 952-966.

Gallup, D.L.: Geochemistry of Geothermal Fluids and Well Scales, and Potential for Mineral Recovery, *Ore Geol. Review*, **12**, (1998), 225-236.

Gordienko, S.P.: Thermodynamic Characteristics of Iron Subgroup Borides, *Powder Metallurgy and Metal Ceramics*, **41:3-4**, (2002), 169-172.

Grafen, H., and Kuron, D.: Pitting Corrosion of Stainless Steels, *Mater. Corros.,* **47**, (1996), 16-26.

Heath, G.R., Heimgartner, P., Irons, G., Miller, R., and Gustafsson, S.: An Assessment of Thermal Spray Coating Technologies for High Temperature Corrosion Protection, *Mater. Sci. Forum,* **251-254**, (1997), 809-816.

Karlsdottir, S.N., and Thorbjornsson, I.O.: Corrosion Testing Down-Hole in Sour High Temperature Geothermal Well in Iceland, NACE Corrosion 2013, paper 2550.

Kaya T., and Hoshan, P.: Corrosion and Material Selection for Geothermal Systems, Proceedings World Geothermal Congress 2005, Antalya, Turkey, 24-29 April 2005.

Klapper, H.S., Baker, M.M., and Baker, M.P.: Scaling and Corrosion Behavior of Metallic Materials after Long-Term Exposure to the Geothermal Fluid of the North German Basin, *NACE Intl. Corros. Conf. Ser.,* **5** (2016), 3470-3478.

Kunitskii, Yu.A., and Marek, E.V.: Some Physical Properties of Iron Borides, *Powder Metallurgy and Metal Ceramics*, **10:3**, (1971), 216-218.

Lichti, K.A., and Yanagisawa, N.: Geothermal Energy Materials and Process Issues, Proceedings World Geothermal Congress 2015, Melbourne, Australia, 19-25 April 2015.

Linter, B.R., and Burstein, G.T.: Reaction of Pipeline Steels in Carbon Dioxide Solutions, *Corros. Sci.,* **41**, (1999), 117-139.

Lopez, D.A., Perez, T., and Simison, S.N.: The Influence of Microstructure and Chemical Composition of Carbon and Low Alloy Steels in CO_2 Corrosion: A State-of-the-Art Appraisal, *Mater. Des.,* **24**, (2003), 561-575.

MacDonald, W.D. and Grauman, J.S.: Development of New Titanium Alloys for Use in Aggressive Geothermal Environments, NACE Corrosion/2019, Paper No. 12871.

Martini, C., Palombarini, G., Poli, G., and Prandstraller, D.: Sliding and Abrasive Wear Behavior of Boride Coatings, *Wear*, **256:6**, (2004), 608-613.

Matkovich, V.I. (Ed.): Boron and Refractory Borides, Springer-Verlag, Berlin, Germany, (1977).

Medvedovski, E., Chinski, F., and Stewart, J.: Wear- and Corrosion-Resistant Boride-Based Coatings Obtained through Thermal Diffusion CVD Processing, *Adv. Eng. Mater.,* **16**, (2014) 713-728.

Medvedovski, E.: Formation of Corrosion-Resistant Thermal Diffusion Boride Coatings, *Adv. Eng. Mater.,* **18**, (2016), 11-33.

Medvedovski, E., J. Jiang, and Robertson, M.: Iron Boride-Based Thermal Diffusion Coatings for Tribo-Corrosion Oil Production Applications, *Ceram. Int.,* **42**, (2016), 3190-3211.

Meier, G.H., Cheng, C., Perlkins, R.A. and Bakker, W.: Diffusion Chromizing of Ferrous Alloys, *Surf. Coat. Technol*., **39-40**, (1989), 53-64.

Miller, R.L.: Chemistry and Materials in Geothermal Systems, in: Casper, L.A, Pinchback, T.R. (Eds.), Geothermal Scaling and Corrosion, **717**, ASTM Special Techn. Publ., (1980), 3-10.

Mittemeijer E.J., and Somers, M.A.J. (Eds): Thermochemical Surface Engineering of Steels. 1st Ed.; Elsevier – Woodhead Publishing: Cambridge, UK, (2014)

Movchan, B.A.; and Yu, Y.K.: High-Temperature Protective Coatings Produced by EB-PVD, *J. Coat. Sci. Technol.*, **1:2**, (2014), 96-110.

Muller, J., Bilkova, K., Genter, A., and Seiersten, M.: Laboratory results of corrosion tests for EGS Soultz geothermal wells, Proceedings World Geothermal Congress 2010, Bali, Indonesia, 25-29 April 2010.

Mundhenk, N., Huttenloch, P., Sanjuan, B., Kohl, T., Steger, H., and Zorn, R.: Corrosion and Scaling as Interrelated Phenomena in and Operating Geothermal Power Plant, *Corros. Sci.,* **70**, (2013), 17-28.

Musil, J., Vlcek, J., and Zeman, P.: Hard Amorphous Nanocomposite Coatings with Oxidation Resistance above 1000°C, *Adv. Appl. Ceram*., **107:3**, (2008),149-154.

Nicholls, J.R.: Designing Oxidation-Resistant Coatings, *JOM*, **52**, (2000), 28–35.

Petrova, R.S., Suwattananant, N., Pallegar, K.K., and Vangaveti, R.: Boron Coating to Combat Corrosion and Oxidation, *Corrosion Rev.,* **25:5-6**, (2007), 556-569.

Regenspurg, S., Feldbusch, E., Byrne, J., Deon, F., Driba, D.L., Henninges J., Kappler, A., Naumann, R., Reinsch, T., and Schubert, C.: Mineral Precipitation during Production of Geothermal Fluid from a Permian Rotliegend Reservoir, *Geothermics*, **54**, (2016), 122-135.

Roberge, P.R.: Handbook of Corrosion Engineering, 2nd ed.; McGraw-Hill Education: New York, USA, (2012).

Samsonov, G.V., and Vinitskii, I.M.: Refractory Compounds: Handbook, 2nd ed., Metallurgia, Moscow, USSR, (1976) (in Russian).

Schreiber, J., Ravier, G., Sontot, O., Hensch, C., and Genter, A.: In situ material studies at high temperature skid (HTS) bypass system of the geothermal power plant in Soultz-Sous-Forets, France, Proceedings, 38th Workshop on Geothermal Reservoir Engineering, Stanford University, Stanford, CA, February 11-13, 2013, SGP-TR-198.

Tabur, M., Izciler, M., Gul, F., and Karacan, I.: Abrasive Wear Behaviour of Boronized AISI8620 Steel, *Wear*, **266:11-12**, (2009), 1106-1112.

Telle, R., Sigl, L.S., and Takagi, K.: Boride-Based Hard Materials; in *Handbook of Ceramic Hard Materials;* R. Riedel (Ed.), Wiley, Weinheim, (2000), 802-945.

Thorbjornsson, I.O., Karlsdottir, S.N., Einarsson, A., and Ragnarsdottir, K.R.: Materials for Geothermal Steam Utilization at High Temperatures and Pressure, Proceedings World Geothermal Congress 2015, Melbourne, Australia, 19-25 April 2015.

Valdez, B., Schorr, M., Quitero, M., Carrillo, M., Zlatev, R., Stoytcheva, M., and De Dios Ocampo, J.: Corrosion and Scaling at Cerro Prieto Geothermal Field, *Anti-Corr. Method Mater.,* **56**, (2009), 28-34.

Wang, D., and Bierwagen, G.P.: Sol–Gel Coatings on Metals for Corrosion Protection, *Prog. Org. Coat*., **64:4**, (2009), 327-338.

Wolframm, M., Rauppach, K, and Thorwart, K: New Mineral Formations and Transport of Particles in the Thermal Water Loop of Geothermal Plants in Germany, *Z. Geol. Wiss.,* **39**, (2011), 213-239.

Yusoff, N., Ko, M., Lichti, K., and Julian, R.: Sulfuric Acid Corrosion of Nickel Base Alloys and Tantalum at 225C, 18th International Corrosion Congress, November, Perth, Australia, (2011).

Zarrouk, S.J., Woodhurst, B.C., and Morris, C.: Silica Scaling in Geothermal Heat Exchangers and Its Impact on Pressure Drop and Performance: Weirakel Binary Plant, New Zealand, *Geothermics*, **51**, (2014), 445-459.